Aerosol and Air Quality Research, 15: 504–516, 2015

ISSN: 1680-8584 print / 2071-1409 online
doi: 10.4209/aaqr.2014.01.0021

Particulate Characterization and Size Distribution in the Exhaust of a Gasoline Homogeneous Charge Compression Ignition Engine

Avinash Kumar Agarwal[1*], Tarun Gupta[2], Jithin Lukose[1], Akhilendra Pratap Singh[1]

[1] *Engine Research Laboratory, Department of Mechanical Engineering, Indian Institute of Technology Kanpur, Kanpur-208016, India*
[2] *Department of Civil Engineering, Indian Institute of Technology Kanpur, Kanpur-208016, India*

ABSTRACT

Agglomeration, coagulation, surface condensation, adsorption and oxidation processes are a part of particulate evolution process and lead to significant changes in characteristics of particulate matter (PM), when they enter the atmosphere. PM formation can be significantly reduced by advanced combustion concepts such as homogeneous charge compression ignition (HCCI). In the present study, experiments were performed in a modified gasoline fuelled HCCI engine at varying intake air temperatures (T_i), exhaust gas recirculation (EGR) rates and relative air-fuel ratios (λ). For particulate characterization, a partial flow dilution tunnel was used to collect particulate samples on a filter paper. These particulate samples were analysed for benzene soluble organic fraction (BSOF), trace metals, and particulate morphology using scanning electron microscopy (SEM). Physical characterisation of particulates was done using engine exhaust particle sizer (EEPS), which measured the particle size-number distribution. In the experiments, higher PM was found for richer fuel-air mixtures and it further increased with application of EGR. Trace metals were found to be significantly lower for HCCI generated PM, which increased with increasing EGR. BSOF was negligible as compared to total PM which showed relatively lower toxicity of gasoline HCCI particulates. Total number of particles reduced with increasing λ, however particulate size-number distribution curve shifted away from accumulation mode, indicating that the particulate size decreased with increasing λ. Higher particle size-number distribution and particle size-mass distribution were observed for increasing T_i. Particulate surface area and volume also increased with increasing T_i and mixture strength.

Keywords: Gasoline HCCI; Particulate matter (PM); Benzene soluble organic fraction (BSOF); Trace metals; Particle size-number distribution.

INTRODUCTION

Diesel and gasoline engines are biggest anthropogenic contributors to urban air pollution in most cities throughout the world. Epidemiological studies link urban fine particles to the adverse health impacts, including increased morbidity and mortality in humans, causing respiratory and cardiac diseases (Schwartz and Marcus, 1990; Schwartz, 1994; Kunzli *et al.*, 2000; Krzyzanowski *et al.*, 2005; Eastwood, 2008). Due to adverse health effects of these pollutants, increasingly stringent emission standards are mandated worldwide, which require simultaneous reduction in emission of particulate matter (PM) and oxides of nitrogen (NO_x) (Ellinger *et al.*, 2001; Mose *et al.*, 2001). PM emitted from automotive engines consists of soot, ash, sulfates, and soluble organic fraction (SOF) containing unburned fuel, lube oil and other organic components (Agarwal *et al.*, 2010). PM can be collected on quartz filter by filtering the engine exhaust. Using this particulate laden filter, PM can be separated into two fractions (Heywood, 1988; Ferguson and Kirkpatrick, 2001). These fractions have different solubility characteristics in various organic solvents. One fraction cannot be dissolved in any organic solvent, which basically comprises solid carbon material and is termed as soot. Soot causes asthma and other chronic obstructive pulmonary diseases. Soluble organic fraction (SOF) is the other fraction of the PM, which gets dissolved in an organic solvent. This fraction is either adsorbed onto soot surface or condensed onto the quartz filter paper. Tan *et al.* (2004) reported that unburnt fuel, lubricating oil and their thermally synthesized products are the basic constituents of SOF. Gasoline PM largely consists of the higher molecular weight hydrocarbons and other organic substances, which constitute approximately 60–99% of total particulate mass. Gasoline PM also contains small amount of sulphates, mainly in the form of sulphuric acid. Sulphuric acid is formed due to oxidation of combustion

* Corresponding author.
Tel.: +91 512 2597982
E-mail address: akag@iitk.ac.in

generated SO_2 (Nam *et al.*, 2008). Kittelson (2006) suggested that formation of particles in SI combustion is highly dependent on engine operating conditions, compared to diesel combustion. Kayes and Hochgreb (1999) comprehensively examined PM formation in SI engines and found that total mass and number concentration, as well as number weighted mean and mode particle sizes were minimum for nearly stoichiometric fuel-air mixtures. They reported that particulate mass and total number of particles increase with increasing engine load. Johnson *et al.* (2005) found that gasoline engines emit lesser particulate mass as compared to diesel engines however gasoline particulates are significant from number stand-point. Several other researchers demonstrated that the fraction of particles emitted in the nuclei mode is higher in gasoline engines compared to diesel engines (Graskow *et al*., 1998; Maricq *et al*., 1999). Under lean engine operating conditions, elemental carbon or soot does not form in large quantities to be of any serious importance for gasoline engines however it is formed in larger quantities for rich fuel-air mixture combustion. Apart from elemental carbon, there are other compounds present in the fuel and lubricating oil such as sulphur and phosphorus, which are precursors to particulate formation. Due to stringent emission norms, sulphur level in the fuel is reduced which prevents sulphate formation from gasoline engines, however significant amount of sulphur and phosphorus is present in the lubricating oil, which favours particulate formation. Singh *et al.* (2006) investigated the role of lubricating oil in soot deposition and trace metal emissions from an engine operated with exhaust gas recirculation (EGR). In another research, Agarwal *et al.* (2004) found that EGR increases the smoke opacity of engine exhaust which is because of higher particulate formation. Nam *et al.* (2008) and Agarwal *et al.* (2003) reported that wear particles from engine components such as valves, valve seals, piston rings and turbochargers also cause trace metal emissions in particulates such as silicon, calcium, zinc and phosphorus. Quadar and Dasch (1992) suggested that partial combustion products of carbonaceous nature are also formed due to spark plug fouling, which in-turn enhances PM emissions. Rathore *et al.* (2010) developed a surface functionalized activated carbon fiber for controlling the engine out particulate emissions. Organic fraction of particulate originates from partially oxidized/pyrolysed fuel and lubricating oils (Williams *et al*., 1987; Agarwal, 2005). Several researchers have shown that fuel is unlikely to be the only source of the organic fraction and lubricating oil contributes to it great (Abdul-Khalek and Kittelson, 1995; Shin and Cheng, 1997). Logically, this is a function of combustible gas temperature in the vicinity of the cylinder walls, which encourages evaporation of the lubricating oil film from the cylinder walls, as observed for the diesel engines (Gupta *et al.*, 2010). The organic fraction of particulate contains chemical species such as alkanes and alkenes, aldehydes, aliphatic hydrocarbons, PAH and PAH derivatives. Basically, organic fraction of particulate containing neutral and aromatic species turns out to be mutagenic and carcinogenic. The toxic potential of particulate was characterized by evaluating benzene soluble organic fraction (BSOF) of the particulate (Cheung *et al*., 2010; Agarwal *et al*., 2013).

Homogeneous Charge Compression Ignition (HCCI) engine is a concept, wherein PM and NO_x emissions are reduced significantly and simultaneously along with higher engine efficiency (Maurya *et al.*, 2009; Agarwal *et al*., 2013). HCCI is a versatile engine technology offering excellent fuel flexibility because it can be used for various fuels such as diesel, gasoline, gaseous fuels and bio-fuels (Komninos *et al.*, 2007; El-Din *et al.*, 2010; Singh *et al.*, 2012; Singh *et al.*, 2014). In HCCI technology, combustion is initiated by compression heating, followed by auto-ignition of combustible charge at multiple locations. Several researchers have already established excellent NO_x characteristics of HCCI combustion (Canakci, 2008; Maurya *et al.*, 2009). Currently, efforts are directed towards minimization of particulate formation.

Price and Stone (2007) reported a significant concentration of accumulation mode particles in HCCI combustion therefore it was predicted that PM mass emission would not be negligible in HCCI combustion mode. They compared the emission characteristics of conventional SI mode of combustion with HCCI modes of combustion and reported NO_x emissions reduction by a factor of 5 compared to conventional SI mode. The unburned hydrocarbon emissions were 10–20% higher than conventional SI combustion mode. At the same operating point, the number concentration of nuclei mode particles was relatively lower for HCCI mode but it was relatively higher (by a factor of 2–3) for accumulation mode particles. The concentration of particulates in the accumulation mode (80–90 nm) was between 10^5–10^6 particles/cm^3. However particle in the nuclei mode (10–20 nm) were between 10^6–10^7 particles/cm^3. For a constant engine speed, number and size distribution of PM from the HCCI engine varies with several operational parameters such as valve timings, intake air temperature (T_i), relative air-fuel ratio, engine load and EGR rate. Kaiser *et al.* (2002) investigated particulate emissions of a gasoline fuelled HCCI engine using early direct injection strategy at various fuel injection timings. They found significantly higher accumulation mode particles and low nucleation mode particles in the HCCI combustion as compared to SI combustion.

Although most researchers suggested that HCCI engine produces lower particulate mass, considering the large number of fine particles emitted, the particulate emissions from the gasoline HCCI engine cannot be neglected and it is essential to investigate this aspect comprehensively. Therefore this study was aimed at understanding the nano-particulate emissions from a gasoline fuelled HCCI engine. Large number of researcher have used in-cylinder mixture preparation technique, which results in inhomogeous mixture leading to higher PM emissions, however in present study, port fuel injection strategy is used for attaining superior air/fuel mixture quality. Physical and chemical characterization of particulate, especially for bulk toxicity and trace metals estimation were also done under different engine operating conditions with varying relative air-fuel ratio (λ) and EGR. In case of gasoline fuelled HCCI, intake air temperature (T_i) significantly affects the air fuel mixing hence experiments

were performed with varying intake air temperature. In HCCI combustion, different chemical reactions remain incomplete due to relatively lower in-cylinder temperatures, which result in emission of large number of harmful pollutants such as trace metals, BSOF, polycyclic aromatic hydrocarbons (PAHs) etc. To examine the chemical characteristics of PM, particulate loaded quartz filters were analysed for different trace metals present in engine exhaust. Scanning electron microscopy was also performed on particulate samples collected on the quartz filter paper under various engine operating conditions to understand the particulate morphology.

EXPERIMENTAL SETUP

The schematic diagram of the experimental setup is shown in Fig. 1.

Engine

The experiments were performed on a four-cylinder, four-stroke, water-cooled diesel engine (Mahindra & Mahindra; Load king NEF 3200 TCI). The engine was coupled with an eddy current dynamometer (Dynalec; ECB 200). One of the four cylinders was modified to operate in HCCI combustion mode, while the other three cylinders operated in conventional CI combustion mode. These three cylinders were used to motor the HCCI cylinder. Installations of separate air intake and exhaust lines along with reduction in compression ratio were the main modifications done for attaining HCCI mode. Fuel supply system for HCCI cylinder was modified and manifold injector was installed for preparation of homogeneous charge. The technical specifications of the engine are given in Table 1.

Engine Instrumentation

In the experiments, preheated intake air was used to control the start of combustion and rate of heat release (RoHR). For this purpose, an external heater was installed and its temperature was precisely controlled using a proportional integral derivative (PID) controller. The air flow rate was measured by using hot film air mass meter (Bosch; HFM5). Gasoline was supplied to port fuel injector by a 12 V DC low pressure fuel pump, which was installed inside the fuel tank. Gasoline was injected at 3 bar pressure in the intake manifold of the HCCI cylinder, where it forms homogeneous mixture with preheated air. Homogeneous mixture strength was controlled by varying the quantity of injected fuel at constant air flow rate. Injected fuel quantity and fuel injection timings were precisely controlled by a microprocessor (National Instruments, cRIO-9014) (compact-RIO Reconfigurable input-output). The signals from the precision shaft encoder, (BEI; H25D-SS-2160-ABZC), air mass meter and pressure transducer were given to the microprocessor. These signals were further processed using a LabVIEW based program, which was designed for online monitoring, processing and recording of various data-sets acquired from the engine. For controlling the HCCI mode, a fraction of exhaust gas was recirculated to the intake manifold through an EGR damper. The EGR rate was measured using an orifice plate and a U-tube manometer installed in the EGR circuit. Rate of EGR was controlled by an EGR valve.

Particulate Sampling Procedure

Particulate samples were collected iso-kinetically using a partial flow dilution tunnel. This tunnel was used to simulate ambient environmental conditions for particulate development, growth, agglomeration, and adsorption processes before particulate collection from the exhaust gas stream. It draws a fraction of exhaust gas from the main

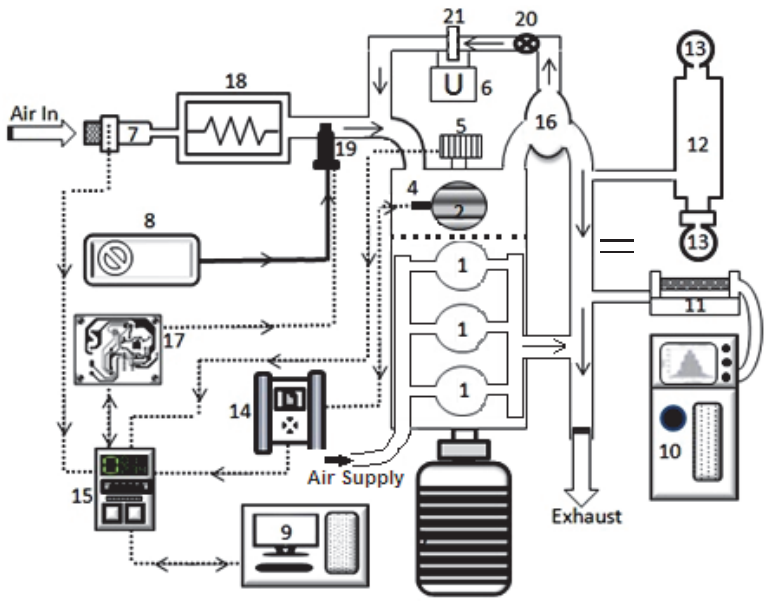

1- CI Mode Cylinder
2- HCCI Mode Cylinder
3- Eddy Current Dynamometer
4- Piezoelectric Pressure Transducer
5- Precision Shaft Encoder
6- U-tube Manometer
7- Laminar Flow Element
8- Fuel Tank & Fuel Pump
9- Data Acquisition Computer
10- Engine Exhaust Particle Sizer
11- Thermo-Diluter
12- Partial Flow Dilution Tunnel
13- Blower
14- Charge Amplifier
15- Micro-Controller for Fuel Injectors
16- Exhaust Plenum
17- Injector Control Circuit
18- Air Preheater
19- Fuel Injector
20- EGR Control Valve
21- Orifice Meter

Fig. 1. Schematic of the gasoline fuelled HCCI engine experiment.

Table 1. Detailed technical specifications of the test engine.

Make	M&M Ltd., India
Model	Load King NEF 3200 TCI
Number of cylinders	4
Displacement volume	2609 cc
Stroke length	94 mm
Bore diameter	94 mm
Compression ratio (HCCI cylinder)	16.5
Connecting rod length	158 mm
Maximum engine output	53.5 kW (72.7 HP) @ 3200 rpm
Maximum torque	195 Nm @ 1900– 2000 rpm
Number of valves per Cylinder	2

exhaust line and mixes it with pre-filtered (using porous quartz filter paper with a pore size of 30–60 microns), preheated atmospheric air (51°C). The dilution ratio was kept constant at 10:1. For all operating conditions, flow rate of exhaust gas in the partial flow dilution tunnel was maintained constant at 3.47 m^3/hr. Diluted exhaust undergoes complete mixing and particulate formation steps viz. condensation of high boiling point hydrocarbon species in gas phase onto the particulates (heterogeneous condensation) along with adsorption, absorption, agglomeration and coagulation. Residence time in the dilution tunnel was therefore designed in such a manner that these reactions are completed before the exhaust gas reaches quartz filter paper/sampling probe. Finally, particulates were collected on a quartz filter paper for further analyses (Gupta *et al*., 2010; Gangwar *et al*., 2012; Agarwal *et al*., 2013). Sampling was done for 30 minutes under different engine operating conditions.

An electronic filter paper micro-balance (Sartorius; CP2-PF) was used for weighing the de-moisturized filter paper before and after the particulate sampling. Total particulate mass was calculated by the difference in filter paper weights. BSOF content was analysed using a segment of particulate laden filter paper. BSOF mainly consists of pyrolytically generated organic species of fuel and lubricating oil which are adsorbed on to the particulate surface during its growth and evolution process. A plastic scissor was used to cut the filter paper into small pieces, which were kept in a reagent beaker containing 20 mL benzene. This beaker was kept in an ultrasonic bath for 20 minutes and then the samples were decanted and vacuum filtered through a 0.45 μm Millipore filter. The filtrate was collected in a pre-weighed beaker which was covered with a perforated aluminium foil. This beaker was kept in an oven at 40°C for 12–18 hours. As a result, the sample dried completely. Finally, the beaker was weighed again to estimate total BSOF content of the particulate sample (Gangwar *et al.*, 2011).

The concentrations of trace metals present in the exhaust particulates were determined by inductively coupled plasma optical emission spectroscopy (ICP-OES) (Thermo Fischer Scientific; iCAP DUO 6300 ICP). In this technique, simultaneous and sequential analysis of multiple trace elements is possible which makes it very important for engine exhaust particulate characterization. Engine exhaust particle sizer (EEPS) (TSI; 3090) was used for physical characterization of the particulate. EEPS can measure size-number distribution of particulates in the size range of 5.6–560 nm with a resolution of 16 channels per decade (a total of 32 channels). For this measurement, a fraction of exhaust gas was drawn from the main exhaust pipeline and diluted using rotating disc thermo-diluter (Matter Engineering; 379020) in order to lower the particle concentration and bring in within the measurement range of the EEPS. EEPS uses a corona charger to put a predictable charge on each particle, depending on its size and surface area. The charged particles are introduced near the centre of the column. Depending on the mass of the particles, these particles get attracted to one of the several ring type electrometers, which are mounted along the axis of the instrument and transfer their charge to these electrometers. The charge collected by these electrometers is then used to calculate the number of particles of that particular size range. Upto 10 sweeps of these measurements are possible in 1 second. For data storage, EEPS is coupled to a dedicated computer. This system therefore provides information of particle size-number distribution, size-surface area distribution, size-volume distribution or size-mass distribution.

RESULTS AND DISCUSSION

The particulate samples were collected using a partial flow dilution tunnel on a quartz filter paper. These particulate laden filters were analysed for BSOF, trace metals and morphology. For particulate characterization, gasoline HCCI experiments were carried out at varying relative air-fuel ratios (λ) and EGR rates.

Particulate Mass Emission and BSOF

The exhaust samples were collected on a quartz filter paper for 30 minutes under different engine operating conditions for analysing the effect of HCCI engine operating parameters on particulate characteristics. In this study particulate emissions cannot be expressed in g/kWh because HCCI experiments were performed in only one cylinder of the modified engine and the remaining three cylinders were operated in conventional CI combustion mode. This led to difficulty in estimating brake power output from each individual cylinder hence it is not feasible to estimate particulate mass emissions from HCCI cylinder. The results of particulate mass (mg) collected on the quartz filter paper in 30 minutes sampling duration under identical sampling

conditions gives a reasonably good idea about the relative particulate emissions. Fig. 2 shows the trend of particulate mass collected on the filter paper with increasing λ at three different EGR conditions. As λ increases, the mixture becomes leaner therefore lower fuel quantity is injected, which leads to lower PM mass emissions. EGR was used to control the RoHR in HCCI combustion but it leads to a NO_x-PM trade-off. Fig. 2 shows that particulate mass emission increases with increasing EGR rate, which is because of lower in-cylinder temperatures due to higher EGR. As a consequence, increase in EGR leads to lower NO_x emissions and higher PM mass emissions in HCCI combustion also. Highest PM mass emission was found at λ = 2.5 and 30% EGR. Collected particulate samples were then analysed for BSOF but BSOF traces were not found in the particulate samples on the filter papers. This observation is in line with the findings of Kittelson (2006) where they indicated that gasoline fuelled engine has insignificant soluble organic fraction. Since there is no BSOF in the particulates, the size-number and size-mass distribution of particulates move away from the accumulation mode with increasing λ.

Trace Metals

Experiments were conducted on particulate samples collected on the filter paper for determining the trace metals and their variation with changing λ and EGR (Fig. 3). Some of the trace metals were below the detection limit of the instrument. In the present experimental investigation, only those metals are reported which could be measured with 90% confidence level. Ba, Cr, Ca, Fe, Cu, Pb and Ni were found to be important trace metals in the gasoline HCCI particulates.

Fig. 3 shows that for all HCCI engine operating conditions, trace metal content in the particulate increases with increasing λ. Relatively lower in-cylinder temperature prevailing in the combustion chamber of the HCCI engine at higher λ was the main reason for this trend. At λ~2.5, particulate quantity emitted was higher (Fig. 2) therefore when the trace metal concentrations per unit particulate mass were calculated, it becomes they were found to be quite low. With increasing λ, fuel quantity supplied in every cycle was very low therefore significantly lower PM (mass) was formed and the trace metal emission per unit particulate mass at higher λ became relatively higher. Trace metal concentration showed increasing trend with EGR and was observed to be maximum for 30% EGR. High trace metal emissions occur due to recirculation of these trace metals with EGR, which dominates the relatively higher particulate mass formed due to EGR. At lower temperatures, large amount of trace metals were emitted due to inferior combustion. Among the trace metals detected, calcium, barium and iron concentrations were relatively higher compared to other metals. Nickel, chromium and lead were detected in lowest concentrations for all engine operating conditions. Main sources of trace metals in particulates are fuel, lubricating oil, ambient dust and engine wear. Calcium is present in both, lubricating oil as well as gasoline, in the form of oxide (CaO). This is a primary calcium traces in the particulates from gasoline HCCI engine. Ca traces increase with increasing λ due to lesser fuel injected in one an engine cycle, which leads to relatively higher degree of incomplete combustion inside the combustion chamber. Fig. 3 shows an increasing trend of iron traces in the particulates with increasing λ. Iron originates primarily from engine wear. When the mixture is relatively richer, higher particulates mass is generated; thereby reducing the iron concentration in the particulates. Small concentration of nickel is used as an additive in the lubricating oil as Nickel ethoxy-ethylxanthate, in order to improve lubrication quality. During combustion, these additives dissociate to release

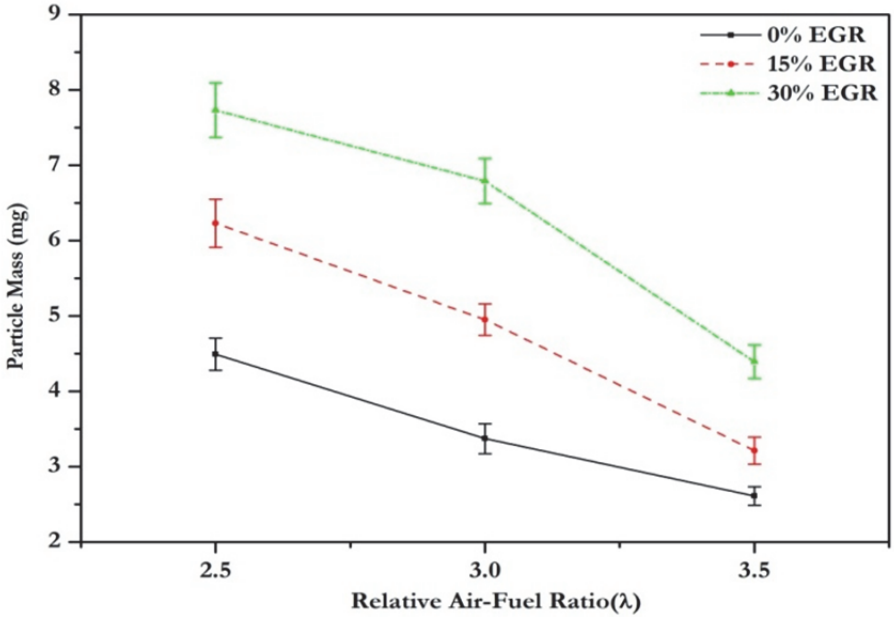

Fig. 2. Particulate mass collected on a quartz filter paper in 30 minutes with varying λ and EGR rates from a gasoline HCCI engine.

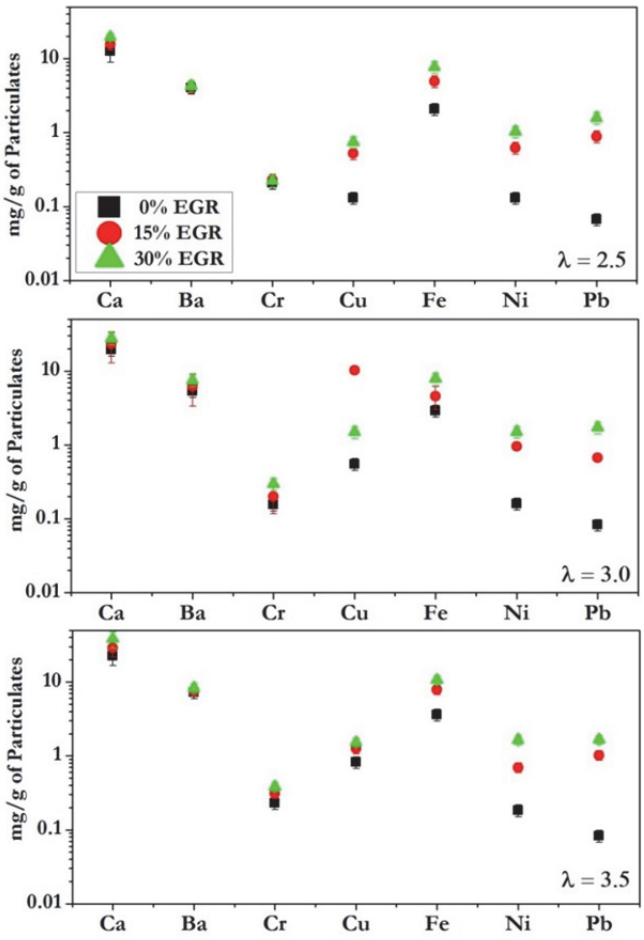

Fig. 3. Trace metals in Gasoline HCCI particulates with varying λ and EGR.

nickel, which is seen as trace metal in the exhaust particulates and has potential harmful health effects for humans. Copper originates from lubricating oil as well as wear of engine components. Copper concentrations in particulates increase with increasing λ (Fig. 3). Chromium and barium originates from the lubricating oil as well as from wear debris of the engine components. Lead was also found in gasoline HCCI particulates as trace metal. Main source of lead is from the small wear debris generated from engine components such as piston and liner. The lead effects most commonly encountered in human population include neurological disorders in children and cardiovascular symptoms (e.g., high blood pressure and heart disease) in adults (Dwivedi *et al.*, 2006).

Particulate Number- Size Distribution

Number and size distribution of particulate emitted was measured using EEPS. In the present investigation, physical analysis was performed at different λ (ranging from 2.4 to 2.8) and varying intake air temperatures (T_i = 140, 150 and 160°C) because both parameters significantly affect the combustion quality. Fig. 4 shows relatively higher number concentration of particulates at lower λ and vice-versa. Combustion of higher fuel quantity inside the engine combustion chamber leads to formation of higher particulate mass (Fig. 2). This effect is also seen in the particulate number-size distribution (Fig. 4).

The peak of the graph starts in the nano-particle region (Dp < 50 nm) and moves upto ultra-fine region (Dp < 100 nm). Experiments show that particle size became finer and the number concentration decreased for leaner mixtures. Particle number concentration increased with increasing T_i however particle size reduced with higher intake air temperature. T_i affected the nano-particles significantly and nano-particle number concentration increased with increasing T_i. However nano-particle concentration was less affected with variations in λ. Large number of particulates at lower λ can be correlated to higher interaction between fuel and air inside the combustion chamber. The particulate number concentration ranges from 6×10^6 to 1.7×10^7 particles/cc for all T_i, which is significantly lesser as compared to conventional SI engine (Gupta *et al.*, 2010). Large number of particles were in range of 20–80 nm.

Fig. 5 shows the total particle concentration for different λ and T_i. It clearly indicates that total particle concentration increases with increasing T_i however it reduced with increasing λ. At lower λ, mixture became rich and caused larger amount of unburnt charge to remain trapped in the crevices. However at higher intake temperatures, knocking causes inferior combustion. In both cases, more soot precursors were generated which caused higher number

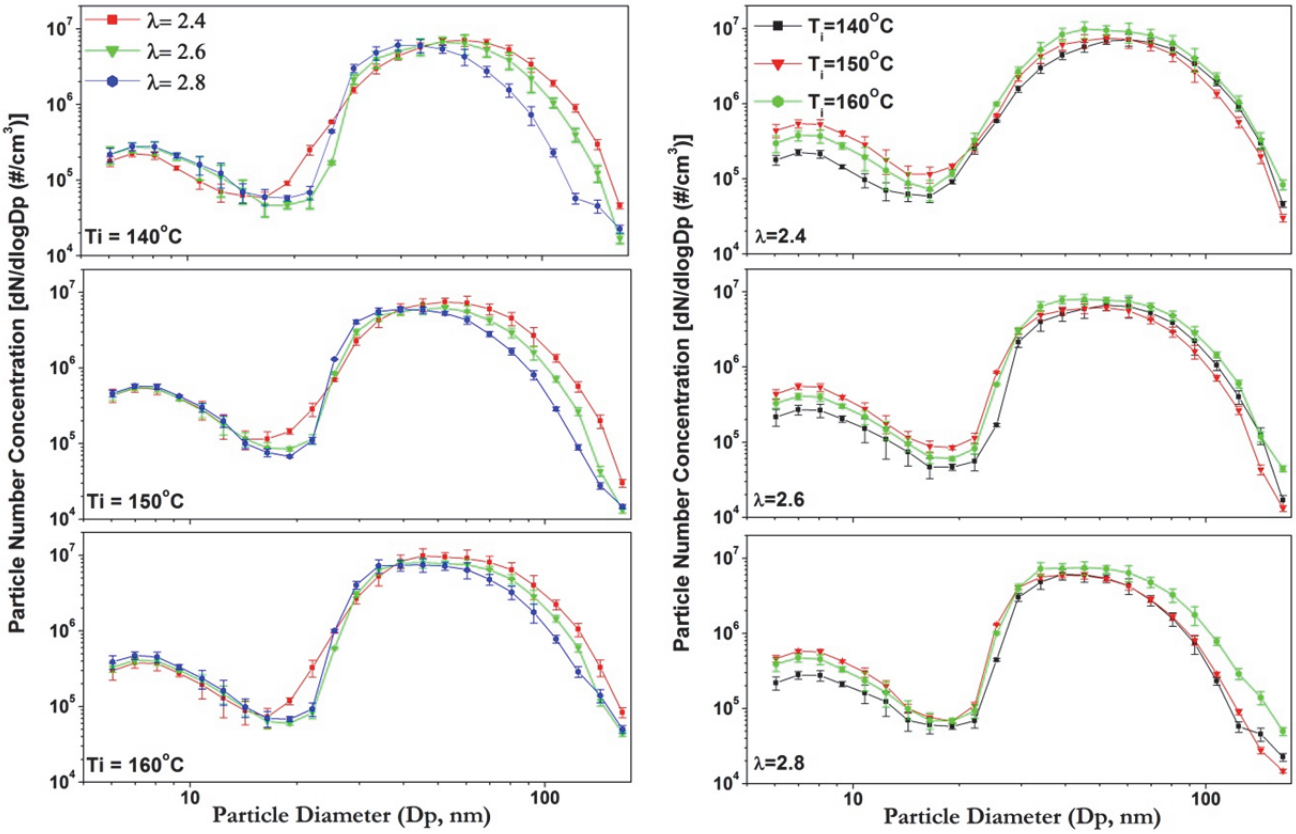

Fig. 4. Particulate size-number distribution for varying λ and T_i in gasoline HCCI engine.

concentration of particles. In all engine operating conditions, total particle concentration ranged from 3.42×10^7 to 6.24×10^7 particles/cc.

Particulate Surface Area-Size Distribution

Fig. 6 shows the surface area-size distribution of the particulates for different values of λ and T_i. Particle surface area was calculated by assuming exhaust particulates to be perfectly spherical.

$$dS = dN.(D_p)^2 \quad (1)$$

where dS is the area concentration of size range with mean diameter D_p and dN is the number concentration of particulates with mean diameter D_p. The surface area vs. size distribution is very important from toxicological point of view. It is a measure of active sites available for adsorption of volatile hydrocarbon species and PAHs. These species are largely toxic species. Particulate surface area distribution is also a measure of interaction between particulates and respiratory system of living beings, which in-turn determines their effect on the health. In the experiments, PM surface area increased with lowering λ, however distribution curve shifted towards left for leaner mixture conditions. At lower temperatures, tendency of condensation of gaseous species (combustion products, unburnt fuel and lube oil) was higher hence particle surface area was also seen to be higher. As T_i increased, particulate surface area slightly reduced due to relatively higher oxidation of soot particles and lesser condensation of combustion products (for 150°C). However at higher T_i (for 160°C), slightly higher surface area distribution was observed due to large particulate concentration, which dominated lower condensation of gaseous products. Surface area of nano-particles was slightly affected by the intake air temperature as well as λ.

Particulate Volume- Size Distribution

Fig. 7 shows the volume size distribution of particulate at different λ and T_i. The volume vs. particle size curve represents the volume of the particles in that particular size range. Harris and Maricq (2002) suggested that particulate volume distribution with size depends on the mean diameter, number and fractal dimensions of the particulates. In the experiments, higher particulate volume was seen for richer mixture conditions however particulate volume slightly increased with increasing T_i. As T_i increased, peak of particulate volume curve shifted towards higher particle size, thus indicating that larger particle volume was contained by ultra-fine range of particulates. However peak of particulate volume curve shifted towards larger size at lower λ. Similar to surface area, volume-size distribution of nano-particle was slightly affected by λ and intake air temperature. In all engine operating conditions, maximum particulate volume went upto 1.12×10^{12} nm^3/cc.

Particulate Mass-Size Distribution

Fig. 8 shows the particulate mass emissions from the engine (μg/m^3 of exhaust gas). T_i and λ, both have profound

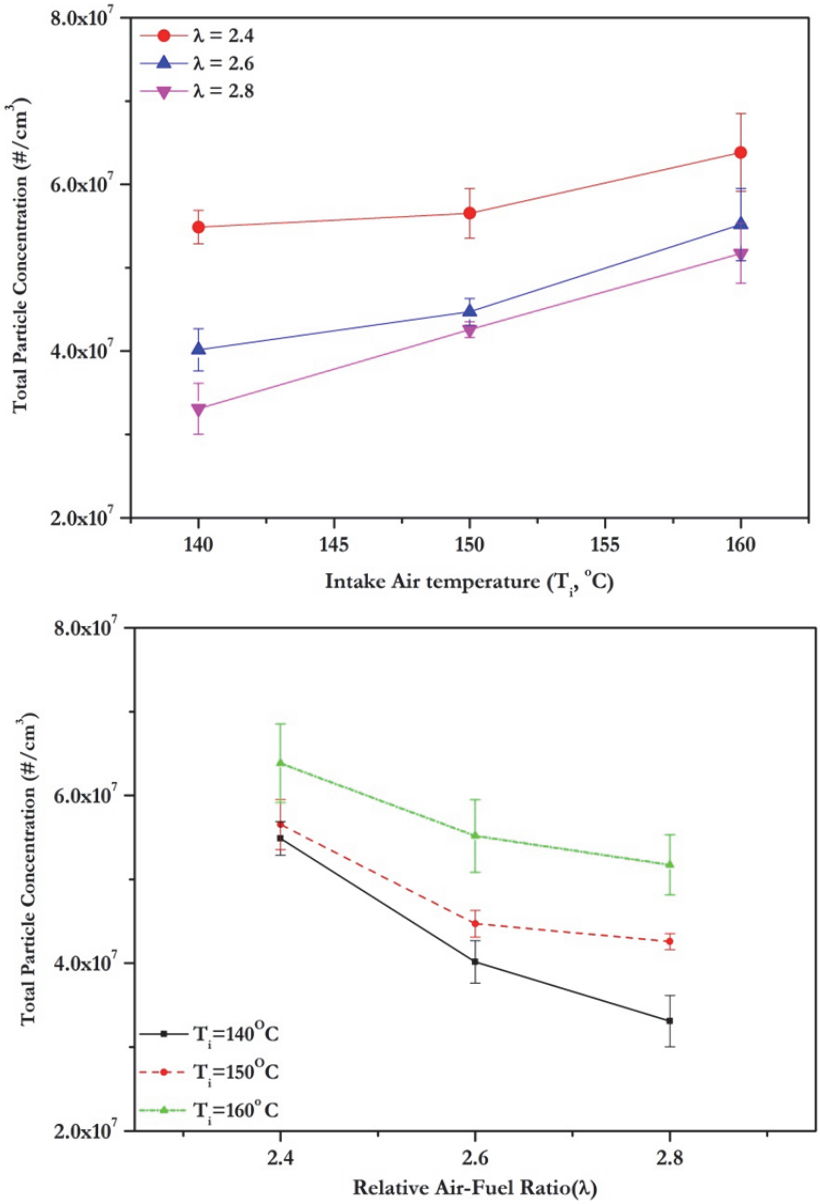

Fig. 5. Total particulate concentration for varying λ and T_i in gasoline HCCI engine.

effects on particulate emission (Fig. 5). If the particulate mass is higher for larger particles then the possibility of their settling down will also be higher because heavier particles tend to settle faster. However tiny particles have higher ambient retention time as compared to larger particles. In these experiments, particulate mass decreased with increasing λ. The particulate mass emission was highest, when the mixture was rich (λ = 2.4), which was approximately 1900 $\mu g/m^3$ of exhaust. Similar trends were obtained by chemical analysis of particulate laden filters (Fig. 2). The curve shifted away from accumulation mode with increasing λ. The particulate mass was low at relatively lower T_i and increased with increasing T_i due to increasing knocking tendency.

Morphology of the Gasoline HCCI Particulate

SEM images were taken for the samples collected on the filter paper (30 min sampling duration) from the partial-flow dilution tunnel for varying λ and EGR. The samples were magnified 1200X and the micrographs of different particulate laden filters are shown in Fig. 9.

Most of the particulate emissions were in the nano-particle range (Figs. 4 and 8); hence it was very difficult to have a comparison of the amount of particulate emitted from the engine. The morphology of the blank filter is shown in Fig. 9; in order to distinguish the particulate emitted by the gasoline HCCI engine. It can be observed that the filter papers were almost clean under all engine operating conditions, except at λ = 2.5 and λ = 3, where some particle agglomerates were observed in these micrographs. One can also observe that the number of particulates collected on the filter paper increased with increasing EGR and these results validated the earlier observations (Fig. 2).

Present study shows the difference between emission characteristics of HCCI engine and conventional CI and SI

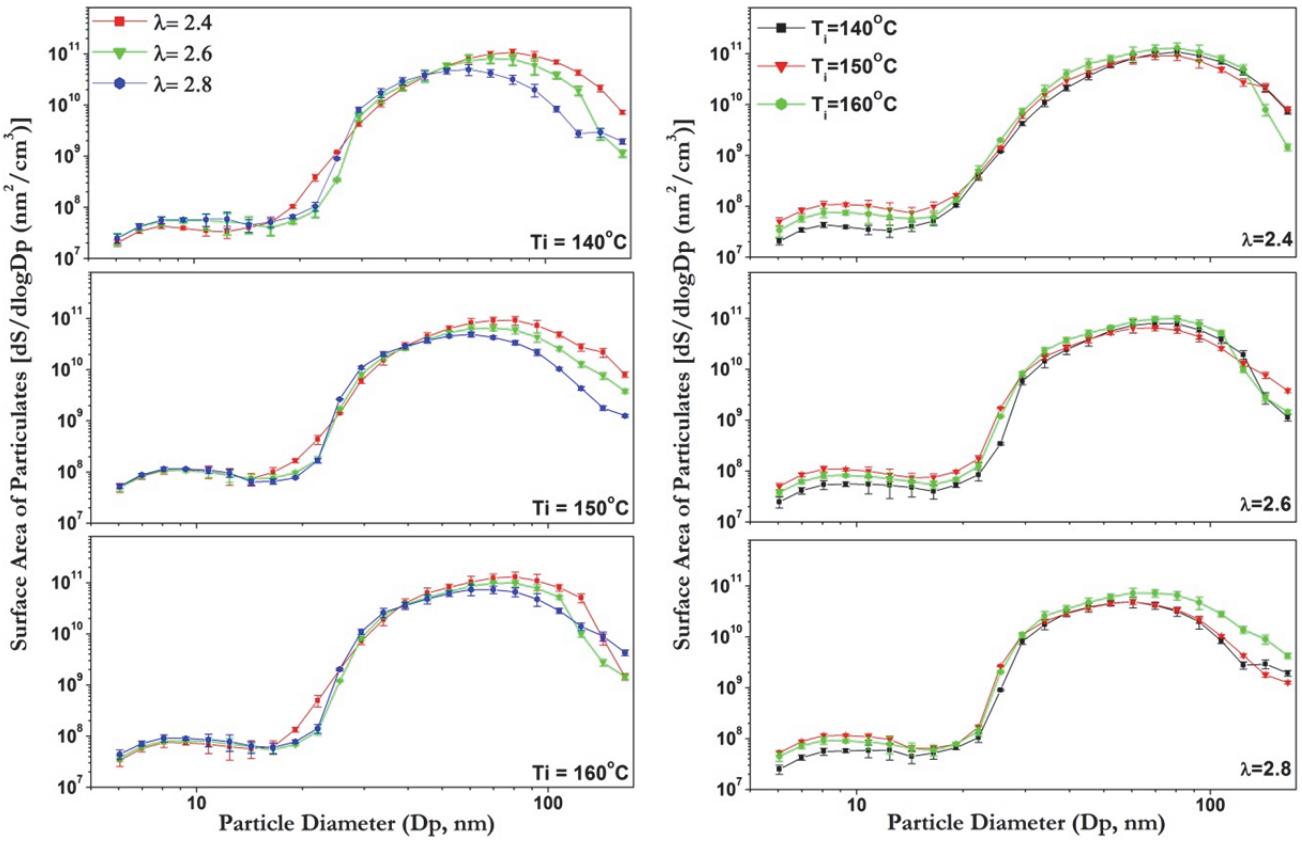

Fig. 6. Particulate surface area-size distribution for varying λ and Ti in gasoline HCCI engine.

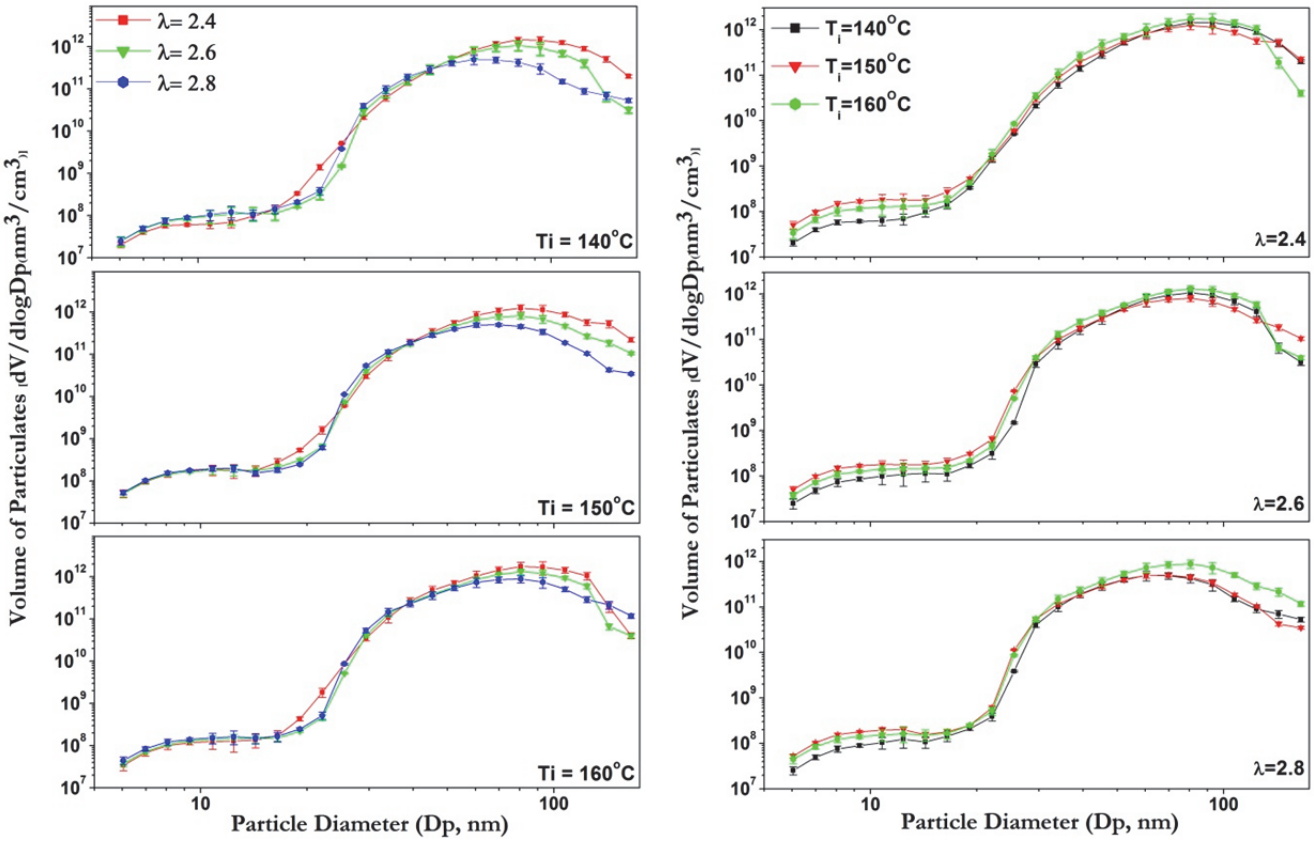

Fig. 7. Particulate volume-size distribution for varying λ and Ti in gasoline HCCI engine.

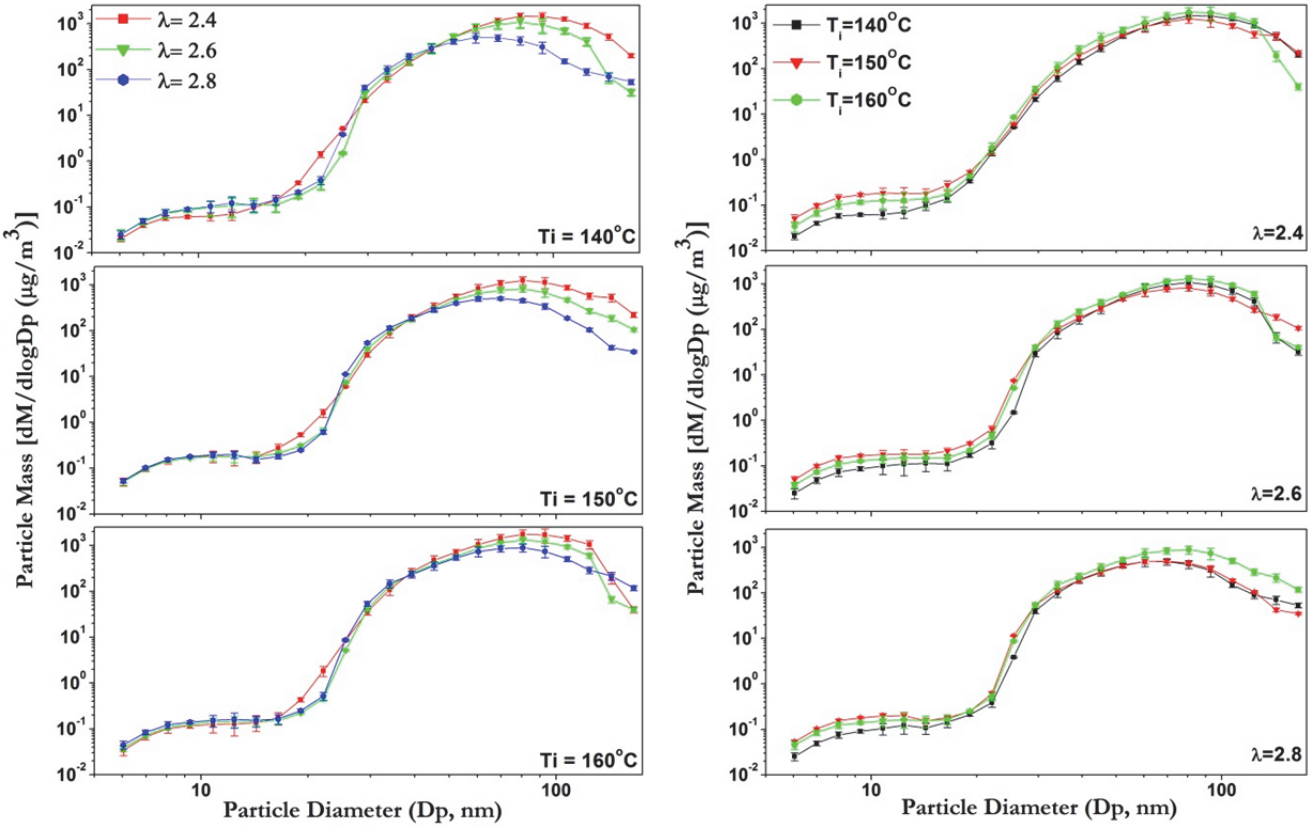

Fig. 8. Particulate mass concentration-size distribution for varying λ and Ti in gasoline HCCI engine.

engines. In conventional CI engines, particle number desnity reaches upto ~10^9 particles/cc (Agarwal *et al.*, 2013) however SI engines emit particle density upto ~5.0 × 10^7 particles/cc (Srivastava *et al.*, 2011). This study shows that gasoline fuelled HCCI engines emit particles within a range of ~7 × 10^6 particles/cc, which is significantly lower compared to conventional engines. Physical characteristics of gasoline HCCI particles are also different from particles emitted in conventional combustion modes. In CI combustion, maximum number of particles emitted are in size range of 100–150 nm however in SI combustion, particle sizes are very low and maximum particle concentration lies in the size range of 20–50 nm. However in gasoline HCCI combustion, most of the particles are in size range of 50–100 nm (between nano-particle range to ultra-fine particle range), which seems to be a distinct property of HCCI engines. Similar particle number-size distribution is also reported for diesel HCCI combustion under similar experimental conditions (Agarwal *et al.*, 2013). Under the same test procedure and experimental conditions, particulate mass is found to be slightly higher for diesel HCCI as compared to gasoline HCCI. BSOF was negligible in gasoline HCCI. Trace metal emission characteristics of diesel HCCI are also different from gasoline HCCI. In gasoline HCCI Ca, Ba, Cu and Fe are the dominating trace metals in particulates however in diesel HCCI Zn, Mn, Fe and Si are found in large proportions in the particulates. SEM images of gasoline HCCI particulate laden filter show lower particle density than diesel HCCI filter, which reflect lower PM emissions from gasoline HCCI.

CONCLUSIONS

Particulate matter (PM) emissions from HCCI engine largely depend on the EGR rate, relative air-fuel ratio (λ) and inlet air temperature (T_i). Particulate mass collected from the dilution tunnel increased with increasing EGR rate and it decreased with increasing λ. The particulate samples were analysed for trace metals (Ca, Fe, Ba, Pb, Cu, Cr and Ni). Most of the trace metals were relatively higher at higher EGR rates. Surface area, volume/mass, number and size distribution of gasoline HCCI exhaust particulates was obtained by engine exhaust particle sizer (EEPS), which validated the above-mentioned statement. It was observed that most of the particles emitted were in the ultra-fine particle size range and their distribution moved away from the accumulation mode particle size range. Total particle concentration reflected the general trend that the particle number concentration increased with increasing T_i however it reduced for leaner mixture conditions. The reason for this trend was negligible BSOF formation in HCCI mode of combustion, which suggested that the gasoline HCCI particulates are inherently less harmful. Particulate surface area distribution curve showed that toxic substance carrying capacity of particulates decreased slightly with increasing T_i however it increased at higher λ. Particulate mass-size distribution was calculated and it validated the results of chemical analysis. Scanning electron

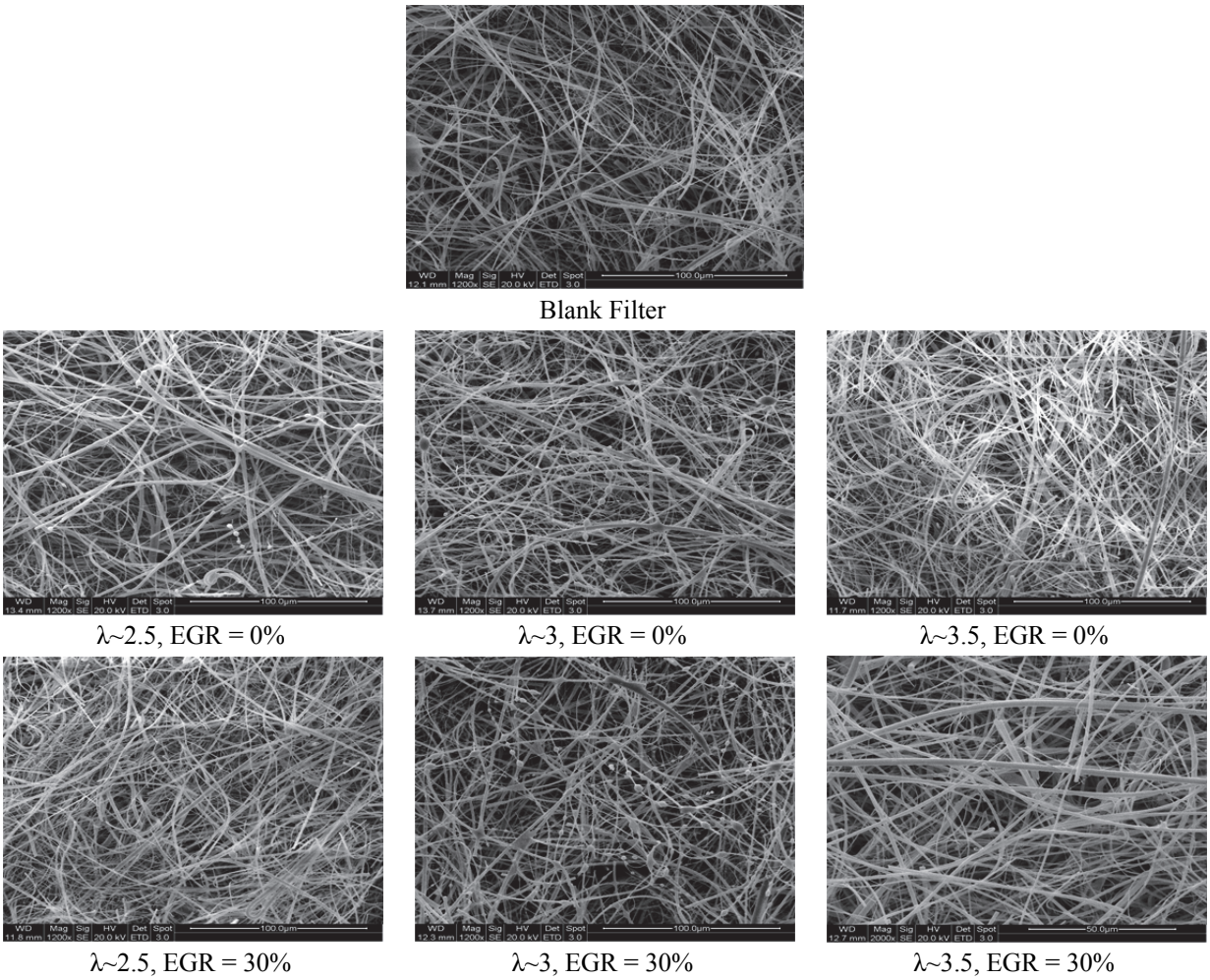

Fig. 9. SEM micrographs of HCCI particulate laden filters vis-à-vis blank filter.

microscopy (SEM) results also verified earlier observations. The SEM images showed that the particulate emissions from the gasoline fuelled HCCI engine were negligible, rendering this combustion mode more environment benign from particulate toxicity point of view.

REFERENCES

Abdul-Khalek, I.S. and Kittleson D.B. (1995). Real Time Measurement of Volatile and Solid Exhaust Particles Using a Catalytic Stripper. *SAE Technical Paper* 950236.

Agarwal, A.K., Bijwe, J. and Das, L.M. (2003). Effect of Biodiesel Utilisation on Wear of Vital Parts in Compression Ignition Engine. *J. Eng. Gas Turbines Power* 125: 604–611.

Agarwal, A.K., Singh, S.K., Sinha, S. and Shukla, M.K. (2004). Effect of EGR on the Exhaust Gas Temperature and Exhaust opacity in Compression Ignition Engines. *Sadhana* 29: 275–284.

Agarwal, A.K. (2005). Lubrication Oil Tribology of a Biodiesel-fuelled CI Engine. *Proc. Inst. Mech. Eng. Part D: J. Automobile Eng.* 219: 703–714.

Agarwal, A.K., Gupta, T. and Kothari, A. (2010). Toxic Potential Evaluation of Particulate Matter Emitted from a Constant Speed Compression Ignition Engine: A Comparison between Straight Vegetable Oil and Mineral Diesel. *Aerosol Sci. Technol.* 4: 724–733.

Agarwal, A.K., Dhar, A., Srivastava, D.K., Maurya R.K. and Singh A.P. (2013). Effect of Fuel Injection Pressure on Diesel Particulate Size and Number Distribution in a CRDI Single Cylinder Research Engine. *Fuel* 107: 84–89.

Agarwal, A.K., Singh, A.P., Lukose, J. and Gupta, T. (2013). Characterization of Exhaust Particulates from Diesel Fuelled Homogenous Charge Compression Ignition Combustion Engine. *J. Aerosol Sci.* 58: 71–85.

Agarwal, A.K., Karare, H. and Dhar, A. (2014). Combustion, Performance, Emissions and Particulate Characterization of a Methanol-gasoline Blend (Gasohol) Fuelled Medium Duty Spark Ignition Transportation Engine. *Fuel Process. Technol.* 121:16–24.

Canakci, M. (2008). An Experimental Study for the Effects of Boost Pressure on the Performance and Exhaust Emissions of a DI-HCCI Gasoline Engine. *Fuel* 87: 1503–1514.

Cheung, K.L., Ntziachristos, L., Tzamkiozis, T., Schauer,

J.J., Samaras, Z., Moore, K.F. and Sioutas, C. (2010). Emissions of Particulate Trace Elements, Metals and Organic Species from Gasoline, Diesel, and Biodiesel Passenger Vehicles and Their Relation to Oxidative Potential. *Aerosol Sci. Technol.* 44: 500–513.

Dwivedi, D., Agarwal, A.K. and Sharma, M. (2006). Particulate Emission Characterization of a Biodiesel vs. Diesel-fuelled Compression Ignition Transport Engine: A Comparative Study. *Atmos. Environ.* 40: 5586–5595.

Eastwood, P. (2008). *Particulate Emission from Vehicles*, John Wiley & Sons Ltd.

El-Din, H., Elkelawy, M. and Yu-Sheng, Z (2010). HCCI Engines Combustion of CNG Fuel with DME and H_2 Additives. *SAE Technical Paper* 2010-01-1473.

Ellinger, R., Prenninger, P., Meitz, K., Brandstatter, W. and Salchenegger, S. (2001). Comparison of CO_2 Emission Levels for Internal Combustion Engine and Fuel Cell Automotive Propulsion Systems. *SAE Technical Paper* 2001-01-3751.

Ferguson, C.R. and Kirkpatrick, A.T. (1986). *Internal Combustion Engine*, John Wiley & Sons, New York.

Gangwar, J.N, Gupta, T. and Agarwal, A.K. (2011). Comparison of Emission from Diesel vs. Biodiesel Fuel Used in CRDI SUV Engine: PM Mass and Chemical Composition Investigation. *Inhalation Toxicol.* 23: 449–458.

Gangwar, J.N, Gupta, T. and Agarwal, A.K. (2012). Composition and Comparative Toxicity of Particulate Matter Emitted from Diesel and Biodiesel Fuelled CRDI Engine. *Atmos. Environ.* 46: 472–481.

Graskow, B., Kittelson D.B., Abdul-Khalek I.S., Ahmadi, M.R. and Morris J.E. (1998). Characterization of Exhaust Particulate Emissions from a Spark Ignition Engine. *SAE Technical Paper* 980528.

Gupta, T., Kothari, A., Srivastava, D.K. and Agarwal, A.K. (2010). Measurement of Number and Size Distribution of Particles Emitted from a Mid-Sized Transportation Multipoint Port Fuel Injection Gasoline Engine. *Fuel* 89: 2230–2233.

Harris, S.J. and Maricq, M.M. (2002). The Role of Fragmentation in Defining the Signature Size Distribution of Diesel Soot. *Aerosol Sci.* 33: 935–42.

Heywood, J.B. (1988). *Internal Combustion Engine Fundamentals*, McGraw-Hill, New York.

Johnson, J.P., Kittelson, D.B. and Watts, W.F. (2005). Source Apportionment of Diesel and Spark Ignition Exhausts Aerosol Using On-road Data from the Minneapolis Metropolitan Area. *Atmos. Environ.* 39: 2111–2121.

Kaiser, E.W., Yang, J., Culp, T., Xu, N. and Maricq M.M. (2002). Homogeneous Charge Compression Ignition Engine-out Emissions-Does Flame Propagation Occur in Homogeneous Charge Compression Ignition? *Int. J. Engine Res.* 3: 185–195.

Kayes, D. and Hochgreb, S. (1999). Mechanisms of Particulate Matter Formation in Spark-ignition Engines. 1. Effect of Engine Operating Conditions. *Environ. Sci. Technol.* 33: 3957–3967.

Kittelson, D.B. (2006). Ultrafine Particle Formation Mechanisms. University of Minnesota Center for Diesel Research, Conference on Ultra-fine Particles: Science, Technology and Policy Issues, April 30–May 2006.

Komninos, N.P., Hountalas, D.T. and Rakopoulos C.D. (2007). A Parametric Investigation of Hydrogen HCCI Combustion Using a Multi-zone Model Approach. *Energy Convers. Manage.* 48: 2934–2941.

Krzyzanowski, M., Kuna-Dibbert, B. and Schneider, J. (2005). Health Effects of Transport-Related Air Pollution, World Health Organization.

Kunzli, N., Kaiser, R., Medina, S., Studnicka, M., Chanel, O. and Filliger, P. (2000). Publichealth Impact of Outdoor and Traffic-related Air Pollution: A European Assessment. *Lancet* 356: 795–801.

Maricq, M.M., Podsiadlik, D.H. and Chase, R.E. (1999). Gasoline Vehicle Particle Size Distributions: Comparison of Steady State, FTP, and US06 Measurements. *Environ. Sci. Technol.* 33: 2007–2015.

Maurya, R.K. and Agarwal, A.K. (2009). Experimental Investigation of Cycle-by-cycle Variations in CAI/HCCI Combustion of Gasoline and Methanol by Varying Different Engine Operating Conditions. *SAE Technical Paper* 2009-01-1345.

Mose, F.X., Sams, T. and Cartellieri, W. (2001). Impact of Future Exhaust Gas Emission Legislation on the Heavy Duty Truck Engine. *SAE Technical Paper* 2001-01-0186.

Nam, E., Fulper, C., Warila, J., Somers, J., Michaels, H., Baldauf, R., Rykowski, R. and Scarbro, C. (2008). Analysis of Particulate Matter Emissions from Light-duty Gasoline Vehicles in Kansas City. U. S. Environmental Protection Agency, EPA420-R-08-010 April 2008.

Price, P., Stone, R., Misztal, J. and Xu, H. (2007). Particulate Emissions from a Gasoline Homogeneous Charge Compression Ignition Engine. *SAE Technical Paper* 2007-01-0209.

Quadar, A.A. and Daschm C.J. (1992). Spark Plug Fouling: A Quick Engine Test. *SAE Technical Paper* 920006.

Rathore, R.S., Srivastava, D.K., Agarwal, A.K. and Verma, N. (2010). Development of Surface Functionalized Activated Carbon Fiber for Control of NO and Particulate Matter. *J. Hazard. Mater.* 173: 211–222.

Schwartz, J. and Marcus, A. (1990). Mortality and Air Pollution in London: A Time Series Analysis. *Am. J. Epidemiol.* 131: 185–194.

Schwartz, J. (1994). Air Pollution and Daily Mortality: A Review and Meta-analysis. *Environ. Res*. 64: 36–52.

Shin, Y. and Cheng, W.K. (1997). Engine-out ‘‘Dry” Particulate Matter Emissions from SI Engines. *SAE Technical Paper* 972890.

Singh, A.P. and Agarwal, A.K. (2012). An Experimental Investigation of Combustion, Performance and Emission from a Diesel HCCI Engine. *SAE Technical Paper* 2012-28-005.

Singh, G., Singh, A.P. and Agarwal, A.K. (2014). Experimental Investigations of Combustion, Performance and Emission Characterization of Biodiesel

Fuelled HCCI Engine Using External Mixture Formation Technique. *Sustainable Energy Technol. Assess.* 6: 116–128.

Singh, S.K., Agarwal, A.K. and Sharma, M. (2006). Experimental Investigations into Lubricating Oil Tribology of EGR Operated Engine. *Appl. Therm. Eng.* 26: 259–266.

Srivastava, D.K., Agarwal, A.K. and Gupta, T. (2011). Effect of Engine Load on Size and Number Distribution of Particulate Matter Emitted from a Direct Injection Compression Ignition Engine. *Aerosol Air Qual. Res.* 11: 915–920.

Tan, P.Q., Deng, K.Y. and Lu, J.X. (2004). Analysis of Particulate Matter Composition from a Heavy-duty Diesel Engine. *Proc. Inst. Mech. Eng. Part D: J. Automobile Eng.* 218: 1325–1331.

Williams, P.T., Andrews, G.E. and Bartle, K.D. (1987). The Role of Lubricating Oil in Diesel Particulate and Particulate PAH Emissions. *SAE Technical Paper* 87084.

Received for review, January 23, 2014
Revised, July 10, 2014
Accepted, September 14, 2014